

Modification of Catalytic Activity of Cu-Ti Amorphous Alloy Ribbons by Cathodic Hydrogen Charging^{*}

by M. Pisarek^{1,2}, M. Janik-Czachor^{1**}, P. Kedzierzawski¹,
Á. Molnár³, B. Rác³ and A. Szummer²

¹*Institute of Physical Chemistry, Polish Academy of Sciences, 01-224 Warsaw, Kasprzaka 44/52, Poland*

²*Faculty of Materials Science and Engineering, Technical University of Warsaw, Warsaw, Poland*

³*Department of Organic Chemistry, University of Szeged, Szeged, Hungary*

(Received April 15th, 2004)

Since hydrogen is known to be one of the most efficient embrittling atomic species, cathodic hydrogen charging was used in an attempt to modify the structure, composition and morphology of Cu-Ti amorphous alloy ribbons. Various methods of analysis such as X-ray electron microanalysis, SEM, XRD and electrochemistry, with varying lateral resolution and different information depths, as well as catalytic tests, were used to follow the changes within the ribbons and at the surface, and their interrelations with catalytic activity. The activity in a test reaction (dehydrogenation of 2-propanol) was enhanced up to a conversion level of 66%, which is much higher than that obtained with all other pre-treatments previously applied.

Key words: Cu-Ti, amorphous alloys, devitrification, Cu segregation, XRD, hydrogen charging, catalytic tests, X-ray microanalysis (WDS), SEM

Investigations of the surfaces of amorphous Cu-Ti alloy ribbons exposed to air at room temperature in a laboratory atmosphere (ageing in air/corrosion), even for several years, have shown that this method does not enhance surface segregation of Cu, and thus appears to be inefficient in transforming a Cu-Ti ribbon precursor into a catalytically active substrate. This behavior, confirming the high stability of Cu-Ti amorphous alloy, is in contrast to that of Cu-Zr and Cu-Hf, which are prone to devitrification and a concomitant Cu-segregation with ageing. In fact, the ease of structural changes of Zr-based amorphous alloys (AAs) induced by various techniques [1,2] has been utilized to transform AAs of low surface area into active and stable catalyst materials.

In addition to the devitrification occurring during ageing [3], an in situ activation, that is, activation under reaction conditions, was shown in numerous cases to be beneficial [4–7]. The interaction of the reacting molecules with the constituents of the alloys may induce segregation and the formation of materials with high specific activity. Hydrogen and oxygen are two highly effective reagents in such processes.

^{*} Dedicated to Prof. Dr. Z. Galus on the occasion of his 70th birthday.

^{**} Corresponding author: e-mail: maria@ichf.edu.pl

Indeed, oxidation of zirconium during reactions was found to be the main driving force in generating an active metal-on-zirconia catalyst of high surface area [6,7].

Hydrogen is one of the most universal embrittling atomic species, responsible for degradation of ductility, toughness and resistance to subcritical crack growth in a variety of crystalline [8,9] and amorphous [10] metals. Hydrogen treatment at high pressure is known in general to bring about significant changes in the bulk and on the surface of amorphous alloys [11–15]. Some Zr and Ti based metallic glasses have been considered as hydrogen storage materials where the potential embrittling effects of “internal” hydrogen are of significant concern [10,16]. Indeed, hydrides of Zr and Ti are easily formed. The H/M atomic ratio even in Zr or Ti-based AAs may attain values as high as 1.4 [11]. The Zr hydrides formed have a higher volume, and the lattice strain generated brings about segregation of Cu to the surface and the formation of a unique surface morphology [11,15,17–20].

The otherwise detrimental deterioration by hydrogen charging of the mechanical properties of amorphous alloys containing Zr or Hf appeared to be beneficial in the process of activation of Cu-Zr or Cu-Hf AA for catalysts [11] and for SERS (Surface Enhanced Raman Scattering) active substrates [22]. Catalytic efficiency with conversions of about 50% was attained for a 60Cu-40Zr amorphous alloy after high-pressure hydrogen charging and subsequent exposure to air [11]. High-resolution microscopic investigations and Scanning Auger Mapping (SAM) suggested that small Cu clusters were attached to the ZrO_2 substrate, that is, a peculiar type of “catalyst on a support” was formed. Thus, there was a large population of Cu with ZrO_2 boundaries available on the surface, which could have a beneficial effect on the catalytic process, providing both “Cu” and “O” active species at the surface for the catalytic process of dehydrogenation of aliphatic alcohols [22,24]. This material proved to be also an excellent SERS substrate. Analysis of the corresponding SERS spectra [22,24] suggests that some electron deficient Cu clusters were present on the surface; their beneficial role in the catalytic process is suspected [22,23]. Moreover, hydrogen charging of Cu-Hf amorphous alloys resulted in a conversion of 88% while the BET specific surface area attained only $7.4 \text{ m}^2/\text{g}$ [25]. Thus, an attempt was made to use hydrogen charging as a possible means of transforming a rather stable Cu-Ti AA into an efficient catalyst. Cathodic hydrogen charging was chosen for its simplicity as a pretreatment procedure. It is known that during electrolytic hydrogen evolution, a part of the adsorbed hydrogen dissolves in a metal lattice. Mismatch of lattice parameters at the metal/hydride boundary for crystalline materials brings about a generation of numerous defects. A similar phenomenon is observed also for AAs.

EXPERIMENTAL

Materials and microscopic examination. Cu samples were prepared from a 0.5 mm thick Cu sheet of 99.99 % purity. 70Cu-30Ti and 60Cu-40Ti amorphous alloy ribbons, 2–4 mm wide and $\sim 40 \mu\text{m}$ thick, freshly cast, or partially devitrified, were used.

The samples were examined with an optical microscope and a scanning electron microscope (HITACHI 3500N). To monitor surface morphology and composition, X-ray microanalysis was performed by using an electron probe X-ray micro analyser (CAMECA SEMPROBE SU-30), equipped with both WDS and EDS (NORAN Voyager 3100) spectrometers. Line and local area analyses (distribution of all the elements) on the sample surfaces on the wheel side of the ribbon, as well as on polished cross sections of the ribbons, were performed at 7 kV and 15 kV. This method provides an information depth of $\sim 1 \mu\text{m}$ at a lateral resolution of $\sim 1 \mu\text{m}$. See elsewhere [3] for details.

X-ray diffraction. Structural changes within the amorphous ribbons due to cathodic hydrogen treatment were followed with a RIGAKU X-ray diffractometer.

Electrochemical pretreatment and investigation. Amorphous samples were hydrogen charged in order to increase their catalytic activity for the dehydrogenation of 2-propanol. Cathodic charging in 0.5 M H_2SO_4 at $i = \text{const}$ up to -200 mA/cm^2 was applied during time intervals from 20 min up to 9 h. Two different options of hydrogen charging were used: – moderate and elevated current density to produce large effects within a short time – low current density (not higher than -2 mA/cm^2) and prolonged but controlled charging time to produce subtle effects. The latter procedure in particular seemed to be most promising, as the investigations of Gebert *et al.* [26,27] show that even very small amounts of hydrogen, introduced at a current density as low as -1 mA/cm^2 , already produce distinct and well resolved crystallization, thus inducing segregation of small, but detectable amounts of the components of the pretreated amorphous alloys [26,27]. Our own recent results have shown that this procedure was efficient in transforming Cu-Hf amorphous alloys into stable, efficient ($\sim 90\%$) and selective ($\sim 95\%$) catalysts [25]. The Cu-Ti samples were then annealed and exposed to air for a prolonged time to desorb hydrogen and to allow the other element to oxidise. The H/M ratio was determined by elemental analysis. Details are given elsewhere [25]. After cathodic charging, the samples were anodically polarized with $dE/dt = 5 \text{ mV/s}$ from $E = -0.2 \text{ V}$ up to $E = +0.2 \text{ V}$ to remove Cu segregated on the surface. This procedure was a kind of a stripping voltammetry [28], which made it possible to examine the amount of Cu by monitoring the anodic charge consumed for the “anodic stripping”. Details are given elsewhere [3]. All potentials are quoted with respect to a saturated calomel electrode (SCE).

Catalytic test. Dehydrogenation of 2-propanol was chosen to test the changes in the catalytic activity of the pretreated Cu-Ti ribbons; this is “a model reaction” for dehydrogenation of aliphatic alcohols. About 10 mg of the as received (aged) or electrochemically pre-treated ribbon samples was loaded into a glass micro reactor. 2-Propanol was fed by a micro feeder into a stainless steel evaporator, where it was mixed with hydrogen (99.999%). Then the gas mixture (2-propanol/hydrogen = 0.018) was introduced into the reactor, which was maintained at 300°C . The total flow rate was 10 ml min^{-1} . The reactor temperature was controlled to an accuracy of 0.5°C by using a microprocessor-based controller (Selftune plus, LOVE Controls). The effluents sampled by a pneumatic gas sampling system were analysed by GC (Shimadzu 8A equipment, thermal conductivity detector, CWAX 20M column, 100°C , 30 ml min^{-1} flow rate of hydrogen carrier gas). Calculations were made using a Data Apex Chromatography Station for Windows 1.5. The specific surface area of Cu^0 was measured with the aid of N_2O titration [29,30], based on the reaction of nitrous oxide with Cu^0 species using the GC pulse method.

RESULTS AND DISCUSSION

Samples activated cathodically at $\geq -10 \text{ mA/cm}^2$. Microscopic examinations of the 70Cu-30Ti amorphous ribbons confirmed their high stability. Only a minute amount of segregated Cu was observed on the wheel side, whereas the free side was smooth. However, some “circular” precipitates could be distinguished (Fig. 1) at the surface. Careful XRD examinations revealed that these precipitates consisted of a Cu_3Ti phase (see Fig. 2). It is worth noting that this phase appeared to be particularly

susceptible to hydrogen absorption. After cathodic hydrogen charging, the Cu_3Ti reflections disappeared in the XRD pattern (Fig. 2). Furthermore, a broad maximum was developed, suggesting a partial amorphisation of these crystalline precipitates, in addition to the broad signal originating from the matrix, which had probably been previously obscured by the strong signal from crystalline Cu_3Ti . Moreover, reflections corresponding to crystalline Cu appeared, suggesting a concomitant segregation of Cu. Because of the Cu_3Ti reflections present in the XRD pattern before hydrogenation, it was not possible to distinguish whether the absorbed hydrogen caused a pronounced expansion of the interatomic distances in the amorphous phase, as was observed *e.g.* for Cu-Zr AA [11].

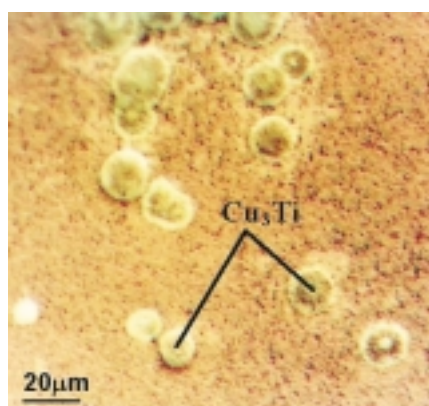


Figure 1. A typical micrograph of a free side of 70Cu-30Ti AA ribbon. Circular second phase branches are distinguishable, corresponding to Cu_3Ti phase.

Cathodic hydrogen charging, in contrast to high pressure hydrogen charging [22], resulted in a peculiar morphology of the segregated Cu on the surface of the ribbon. There is a strong tendency to form a layer of Cu on top of the original ribbon surface. Fig. 3a shows a typical electron microprobe mapping of 70Cu-30Ti surface after cathodic hydrogen charging at $i = -115 \text{ mA/cm}^2$ for 7.5 h. The Cu surface layer is clearly distinguishable; it is rather brittle and thus exhibits a few cracks where the original surface of the AA ribbon is visible underneath. After stripping a part of the Cu layer, a well-developed morphology of its reverse side is visible (Fig. 3b).

In order to quantify the amount of Cu segregated at the surface due to hydrogen charging, anodic Cu stripping was performed. Fig. 4a shows some examples of anodic scans of the ribbon cathodically hydrogen charged previously for 1 h, but at various cathodic current densities ranging from -10 mA/cm^2 up to -200 mA/cm^2 . One can see that, evidently, the higher the cathodic charge used previously for hydrogen charging, the more charge necessary to remove the segregated Cu. These results suggest that there is a close relation between the two phenomena. Indeed, the more hydrogen charging, the more Cu was forced to move to the surface of the ribbon and segregated there. Fig. 4b illustrates the effect of cathodic hydrogen charging on average hydrogen uptake by Cu-Ti AA, as well as on the secondary effect of Cu segrega-

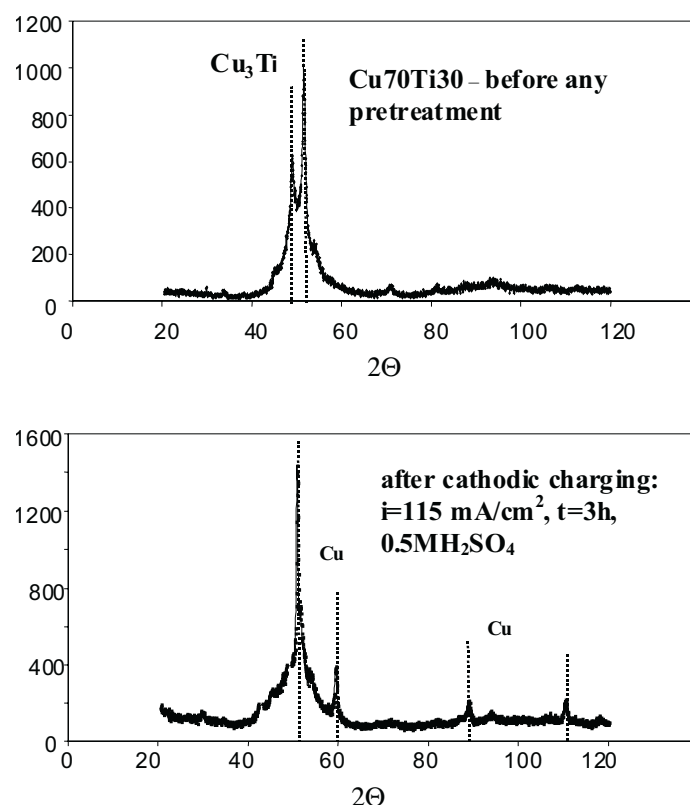


Figure 2. XRD pattern of 70Cu-30Ti ribbon (a) without any pretreatment (b) after cathodic charging. Sharp peaks at $2\theta = 48.8905$ and 51.8874 corresponding to Cu_3Ti phase (embedded into amorphous Cu-Ti alloy) are well distinguishable (a). They disappear after hydrogen charging (b), while, distinct peaks corresponding to crystalline Cu appear.

tion (Q_{cath}) on the ribbon surface due to an engagement of Ti to H. Two options are illustrated in Fig. 4b: charging at a constant current density of -115 mA/cm^2 with time varying from 1 to 8 h, or charging at a constant time equal to 1 h, with current densities varying from 10 to 200 mA/cm^2 . The corresponding values of $Q_{\text{cath}}(t)$ and $Q_{\text{cath}}(i)$ are given in the graph. The amount of Cu segregated during this process is expressed as the amount of charge Q_{Cu} necessary to anodically strip off the Cu layer formed on the ribbon surface (compare Fig. 4a).

Fig. 5 summarises the catalytic activity of the ribbons cathodically hydrogen charged at $i \geq 10 \text{ mA/cm}^2$, as well as those pretreated with hydrogen under high pressure. The effect of the electrochemical method of hydrogen charging was superior, however, only at the beginning of the catalytic reaction. Therefore, more work was definitely needed to further enhance both the activity and stability of the catalyst made from 70Cu-30Ti ribbons. In order to achieve this goal an attempt was made to use low cathodic current density hydrogen charging.

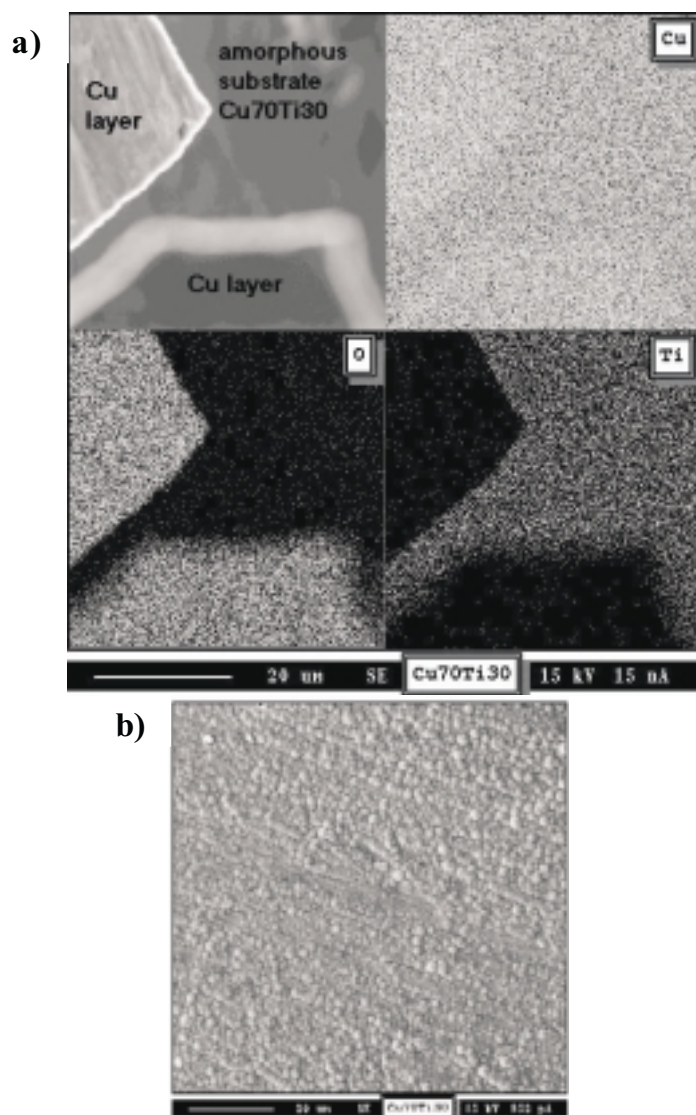


Figure 3. (a) Distribution of Cu (L_{α}), O (K_{α}) and Ti (K_{α}) on the surface of 70Cu-30Ti AA after cathodic charging at $i = -115 \text{ mA/cm}^2$ for 7.5 h; X-ray electron microprobe results. The upper left micrograph shows a secondary electron image of the surface examined by the electron microprobe. (b) Image of the reverse side of the Cu layer stripped from the surface after the cathodic charging; a well-developed rough morphology is visible.

Samples activated cathodically at $i \leq -2 \text{ mA/cm}^2$. Cathodic charging at $i \leq -2 \text{ mA/cm}^2$ resulted in a sample with increased catalytic activity. Under these experimental conditions the segregated Cu exhibited a rather good adhesion to the ribbon. However, morphology, which was considered to be favourable in previous studies [18,22,24,25], was not observed, which indicates, therefore, that a mechanism different from that suggested previously [23] is operative here. Catalytic activity up to 58%

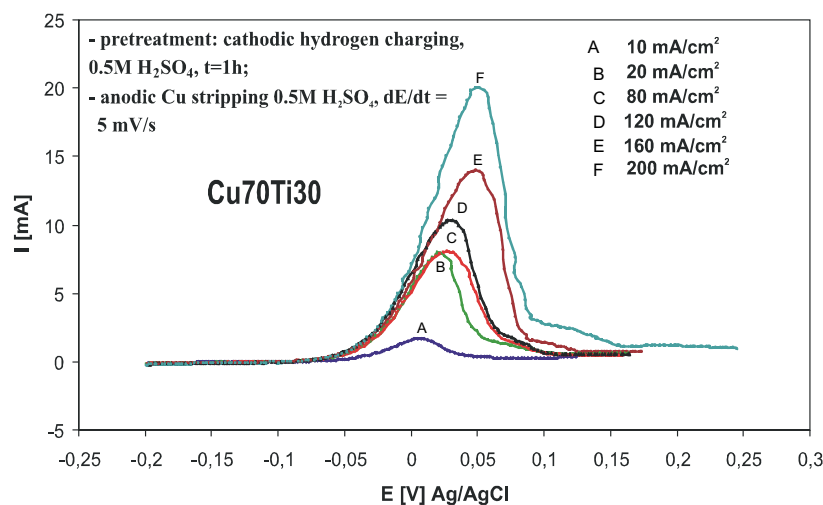


Figure 4a. Current density vs. potential in the course of anodic stripping of the Cu layer formed on the Cu-Ti ribbon during a preceding cathodic hydrogen charging. Cathodic pre-treatment varied from -10 to -200 mA/cm², $t = 1$ h. Anodic Cu stripping at $dE/dt = 5$ mV/s.

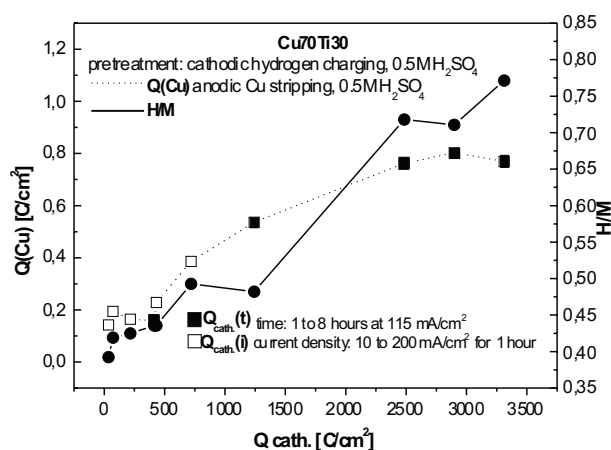


Figure 4b. Effect of cathodic hydrogen charging Q_{cath} on average hydrogen uptake by Cu-Ti AA, as well as on a secondary effect of Cu segregation on the ribbon surface due to engagement of Ti to H. A measure of the amount of Cu segregated during this process is expressed by the amount of charge Q_{Cu} necessary to anodically strip off the Cu layer thus formed on the ribbons surface.

conversion was observed at the beginning, which, however, dropped to 15–20% (see below). Further efforts, therefore, were required to understand the reasons for deactivation. Such understanding may enable the development of catalysts, which retain the initial efficiency for a longer period of the catalytic reaction.

After prolonged hydrogen charging, a sufficient amount of Cu was segregated and was consequently detectable with an X-ray electron microprobe (a morphology similar to that shown in Fig. 3). A careful inspection of the composition maps suggests that after subsequent air exposure Cu was oxidized, as the areas enriched in Ti

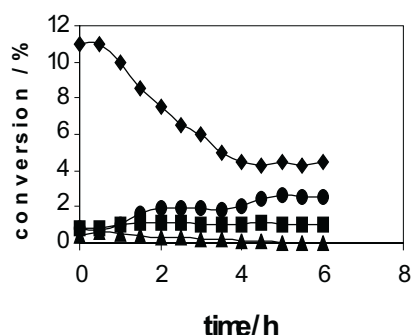


Figure 5. Catalytic activity of Cu₇₀Ti₃₀ AA, presented as conversion vs. time:

- ▲ before any pre-treatment;
- after hydrogen charging at 10 kbar, 70 h, $T = 140^{\circ}\text{C}$;
- after hydrogen charging at 5 kbar, 1 h, $T = 350^{\circ}\text{C}$ (H/M atomic ratio = 0.73);
- ◆ after cathodic charging at $i = 115 \text{ mA/cm}^2$ for 6 h – solution: 0.5 M H_2SO_4 (H/M atomic ratio = 0.45).

coincide with those not enriched in oxygen. This behavior is completely different than that of chemically modified Cu-Zr amorphous alloys where formation of Cu clusters on an oxide support (ZrO_2) was observed after hydrogen charging and air exposure.

Elemental analysis has revealed that the amount of hydrogen in the material was rather high ($\text{H/M} \sim 1.04$) after 52 h of charging at $i = 1 \text{ mA/cm}^2$. It should be emphasized, however, that the local hydrogen content is expected to be substantially different from the average. Hydrogen concentration maximizes at the thin surface layer probably as titanium hydride, which then blocks a further hydrogen entry. It is well known that the diffusion coefficient, such as in Pd hydrides, is several orders of magnitude lower than in the α -phase, mainly because of the interstices blocking effect [31]. Hydrogen charging, therefore, affects primarily the surface layer, which is relevant to catalysis.

Since low current density proved to be useful in increasing catalytic activities, prolonged hydrogen charging from 24 h up to 98 h was applied. Now, stable catalytic activities with conversion values up to 66% could be observed (Fig. 6) at excellent selectivities to acetone formation of about 95%. The suggestion may be made that under the conditions investigated, the unique chemistry of the surface and the porosity induced by hydrogen charging contribute to the excellent catalytic performance observed.

One may surmise that absorption of hydrogen by the amorphous alloy material can create and expand microvoids. These would interact to produce large stresses, which could generate microcracks. If the latter intersect free surfaces, the cracks formed could serve as entry points creating an easy path for hydrogen penetrating into the bulk of the amorphous material in the course of prolonged hydrogen charging. These processes would increase porosity, thereby generating high area surfaces where the catalytic reaction could take place.

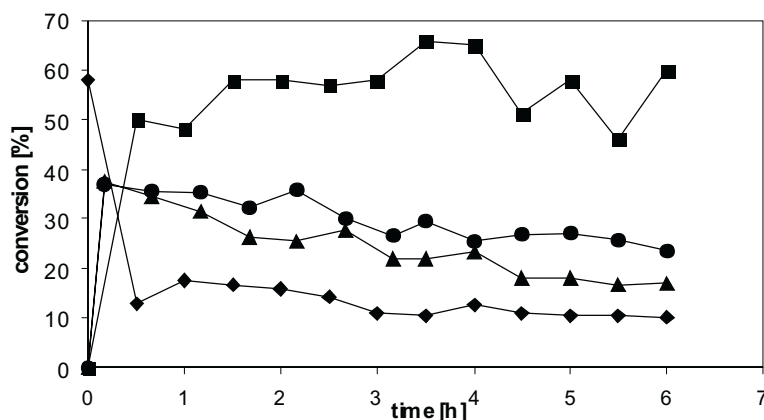
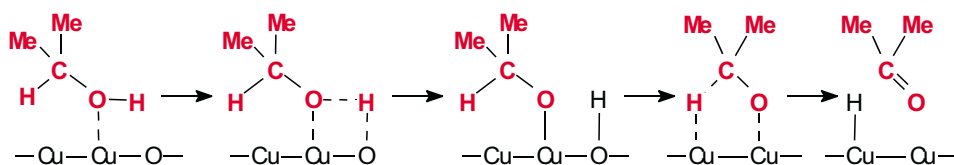


Figure 6. Catalytic activity of Cu-Ti amorphous alloys after cathodic hydrogen charging at low current density ($\leq -2\text{mA}/\text{cm}^2$) over varying charging time from 28 h up to 98 h:

♦ 28 h, ▲ 52 h, ● 72 h, ■ 98 h.

Surface science studies [32] and data acquired by catalytic [33] and kinetic studies [34] indicate that dehydrogenation of alcohols over Cu requires active sites composed of two surface entities. The reacting alcohol chemisorbs on a metallic site (Cu atom) through its O atom, which results in the weakening of the H–O bond (Scheme, showing the process on the example of 2-propanol is given below). Bond breaking leads to the formation of a surface alkoxide group, but the adsorption of hydrogen formed requires the participation of surface oxygen. The surface alkoxide then decomposes by the interaction of a second surface Cu to form adsorbed H and the product carbonyl compound.



–Me stands for methyl radical; $-\text{CH}_3$
Scheme of dehydrogenation of 2-propanol

The catalytic action of the substrate, as above, is a result of partial charge transfer between the various entities on the substrate and in the adsorbed molecule according to the electronegativity of individual atoms.

This mechanism ascribes in fact the weakening of the corresponding 3 bonds in the aliphatic alcohol interacting with 3 surface entities Cu^0 , $\text{Cu}^{\delta+}$ and $\text{O}^{\delta-}$. However, our recent investigations suggest that the mechanism of the catalytic reaction can be different. This suggestion is based on the following experimental results:

- we observed a stable or even increased conversion with time, while the specific copper surface area (Cu^0) is decreasing [11],
- we observed an appreciable, stable conversion of 88% over Cu-Hf [25], while the specific surface area of Cu^0 was zero,
- the present results show that for Cu-Ti conversion reaches 66%, while the segregated Cu layer peels off, and only a minute amount of Cu is present on the surface,
- Cu atoms are necessary to initiate the reaction, as TiO_2 itself exhibits no catalytic activity for the reaction concerned.

A new mechanism should involve interaction of the reacting molecule with $\text{Cu}^{\delta+}$, $\text{Ti}^{\delta+}$, and $\text{O}^{\delta+}$, surface entities. High resolution microscopy and local surface analysis are required to get an insight into the reaction mechanism.

CONCLUSIONS

Cathodic hydrogen charging has been shown to be a superior method of modification of a rather stable 60Cu-40Ti AA. The catalyst thus formed is characterized by high and stable catalytic activity with a maximum conversion of 66%. The outstanding catalytic performance achieved by this pretreatment as well as the characterisation of the catalysts discussed show that the earlier model of the catalytic dehydrogenation of alcohols should be modified in this case.

Acknowledgments

This work was financially supported by the Polish State Committee for Scientific Research (grant KBN 4T08C 025 24) and by the Institute of Physical Chemistry, Polish Academy of Sciences.

REFERENCES

1. Molnár Á., Smith G.V. and Bartók M., *Adv. Catal.*, **36**, 329 (1989).
2. Baiker A., *Glassy metals in catalysis*, in: *Glassy Metals III*, H. Beck, H.-J. Güntherodt, eds., Springer, Berlin, 1994, pp. 121–162.
3. Szummer A., Pisarek M., Dolata M., Molnar A., Janik-Czachor M., Varga M. and Sikorski K., *Mater. Sci. Forum*, 2001, **377**: pp. 15–28.
4. Molnár Á., Katona T., Bartók M. and Varga K., *J. Mol. Catal.*, **64**, 41 (1991).
5. Baiker A., Schlögl R., Armbruster E. and Güntherodt H.-J., *J. Catal.*, **107**, 221 (1987).
6. Schild Ch., Woakun A. and Baiker A., *Surf. Sci.*, **269/270**, 520 (1992).
7. Baiker A., Maciejewski M., Tagliaferri S. and Hug P., *J. Catal.*, **151**, 407 (1995).
8. *Hydrogen Degradation of Ferrous Alloys*, R.A. Oriani, J.P. Hirth and M. Smialowski: (Eds.), Noyes Publication, Park Ridge NJ 1984.
9. Oriani R.A., *Corrosion*, **43**, 390 (1987).
10. Such D., Asoka-Kumar P. and Daukskardt R.H., *Acta Mater.*, **50**, 537 (2002).
11. Szummer A., Janik-Czachor M., Molnar A., Marchuk I., Varga M. and Filipek S.M., *J. Mol. Catal. A Chem.*, **176**, 205 (2001).
12. Baranowski B. and Filipek S.M., *Synthesis of metal hydrides*, in: *High-Pressure Chemical Synthesis*, J. Jurczak, B. Baranowski (Eds.), Elsevier, Amsterdam, 1989, pp. 55–100.
13. Suzuki K., *J. Less Common Met.*, **89**, 183 (1983).

14. Filipek S.M., Szummer A. and Marchuk I., *J. Alloy Compd.*, **293-295**, 7 (1999).
15. Szummer A., Janik-Czachor M., Molnar A., Marchuk I., Varga M. and Filipek S.M., *J. Phys. Condens. Matter.*, **14**, 11405 (2002).
16. Wiswall R., *Hydrogen Storage in Metals*, in: *Hydrogen in Metals II, Application Oriented Properties*, G. Alefeld and J. Volkl (Eds.), Springer-Verlag, Berlin Heidelberg, NJ 1978.
17. Katona T., Molnár Á., Perczel V.I., Kopasz Cs. and Hegedűs Z., *Surf. Interface Anal.*, **19**, 519 (1992).
18. Vanini F., Buechler St., Yu X.N., Erbudak M., Schlappbach L. and Baiker A., *Surf. Sci.*, **189-190**, 1117 (1987).
19. Gasser D. and Baiker A., *Appl. Catal.*, **48**, 279 (1989).
20. Baiker A., Baris H. and Güntherodt H.J., *Chem. Commun.*, 930 (1986).
21. Kudelski A., Janik-Czachor M., Bukowska J., Pisarek M. and Szummer A., *Mater. Sci. Eng.*, **A326**, 364 (2002).
22. Janik-Czachor M., Szummer A., Bukowska J., Molnar A., Mack P., Filipek S.M., Kedzierzawski P., Kudelski A., Pisarek M., Dolata M. and Varga M., *Appl. Catal. A Gen.*, **235**, 157 (2002).
23. Bartók M., et al., *Stereochemistry of Heterogeneous Metal Catalysis*, Wiley, Chichester, 1985, p. 297.
24. Kudelski A., Janik-Czachor M., Pisarek M., Bukowska J., Mack P., Dolata M. and Szummer A., *Surf. Sci.*, **507-510**, 441 (2002).
25. Pisarek M., Janik-Czachor M., Gebert A., Molnár Á., Kędzierzawski P. and Rác B., *Appl. Catal. A: Gen.*, **267**, 1 (2004).
26. Ismail N., Uhlemann M., Gebert A. and Eckert J., *J. Alloy Compd.*, **298**, 146 (2000).
27. Ismail N., Gebert A., Uhlemann M., Eckert J. and Schultz L., *J. Alloy Compd.*, **314**, 170 (2001).
28. Galus Z., *Fundamentals of Electrochemical Analysis 2-nd edn*, Ellis Horwood New York London Toronto Sydney Tokyo Singapore, PWN Warsaw, 1994, p. 518, F. Vydra, K. Štulík and E. Juláková, *Electrochemical Stripping Analysis*, Horwood, Chichester, 1976.
29. Evans J.W., Wainwright M.S., Bridgewater A.J. and Young D.J., *Appl. Catal.*, **7**, 75 (1983).
30. Denise B., Sneed R.P.A., Beguin B. and Cherifi O., *Appl. Catal.*, **30**, 353 (1987).
31. Majorowski S. and Baranowski B., *J. Phys. Chem. Solids*, **43**, 1119 (1982).
32. Madix R.J., *Adv. Catal.*, **29**, 1 (1980).
33. Cunningham J., Sayyed G.H., Cronin J.A., Fierro J.L.G., Healy J., Hirschwald W., Ilyas M. and Tobin J.P., *J. Catal.*, **102**, 160 (1986).
34. Han Y., Shen J. and Chen Y., *Appl. Catal. A Gen.*, **205**, 79 (2001).